Revision 1

Structural complexity of lead silicates: crystal structure of $Pb_{21}[Si_7O_{22}]_2[Si_4O_{13}]$ and its comparison to hyttsjöite

Oleg I. Siidra, Dmitry S. Zenko, Sergey V. Krivovichev*

Department of Crystallography, St. Petersburg State University, 7–9 University Emb., St. Petersburg 199034, Russia

* Corresponding author. E-mail: skrivovi@mail.ru

Abstract

The crystal structure of $Pb_{21}[Si_7O_{22}]_2[Si_4O_{13}]$ has been solved on crystals grown by crystallization from melt. The compound is hexagonal, $P6_3/m$, a = 9.9244(5), c = 34.2357(16) Å, V = 795.28(6) Å^3, R_1 = 0.042 for 3361 unique observed reflections. The structure contains five symmetrically independent Si sites tetrahedrally coordinated by O atoms. The $Si1O_4$, $Si3O_4$ and $Si4O_4$ tetrahedra share corners to form branched heptameric $[Si_7O_{22}]^{16-}$ units, whereas the $Si2O_4$ and $Si5O_4$ tetrahedra form the tetrameric $[Si_4O_{13}]^{10-}$ anions. The structure contains six symmetrically independent Pb sites with the PbO_n coordination polyhedra distorted due to the stereochemical activity of the lone electron pairs. The structure can be described as a stacking of layers of the two types, A and B. The A-type layer contains $[Si_7O_{22}]^{16-}$ units, Pb1, Pb2, Pb3, and Pb4 sites, whereas the B-type layer contains $[Si_4O_{13}]^{10-}$ anions, together with Pb5, Pb6, and Pb6A sites. Stacking of the layers can be described as a sequence ...AA'BAA'B..., where A and A' denote A layers with opposite orientations of the tripod-shaped silicate heptamers. The crystal structure of $Pb_{21}[Si_7O_{22}]_2[Si_4O_{13}]$ has many similarities to that of

hyttsjöite, which contains the same layers consisting of tripod-shaped $[Si_7O_{22}]^{16-}$ anions. In both title compound and hyttsjöite, the anions are stacked together in such a way that ellipsoidal cavities with dimensions of ca. 10×6×6 $Å^3$ are created. The cavities are occupied by the $ClPb_6$ octahedra in hyttsjöite and by 'empty' Pb_6 octahedra in $Pb_{21}[Si_7O_{22}]_2[Si_4O_{13}]$. Analysis of structural and chemical complexity in the PbO-SiO_2 system indicates that the most chemically complex phases (in terms of complexity of relations between chemical components) appear to be the most complex from the structural point of view as well. The title phase is the most structurally and chemically complex phase in the system. Structural organization of crystalline phases in the PbO-SiO_2 system can be described is controlled by the Pb:Si ratio. For the phases with Pb:Si < 2, their structures contain Pb^{2+} ions and silicate anions. For the phases with Pb:Si ≥ 2, the structures contain 'additional' O atoms, i.e. atoms that are not bonded to Si. These atoms form OPb_4 tetrahedra, which are the next strongest structural subunits in the structure after silicate anions. The structures of the phases with Pb:Si < 2 can therefore be described as based upon silicate anions and polynuclear cationic units consisting of edge- and corner-sharing OPb_4 tetrahedra.

Keywords: lead silicate; new mineral; crystal structure; hyttsjöite; lone electron pair stereoactivity; structural complexity.

Introduction

Within recent years, a number of novel Pb-containing silicate mineral species have been reported in the literature (Chukanov et al. 2008; Yakubovich et al. 2008; Kampf et al. 2009; Belokoneva and Dimitrova 2011; Kolitsch et al. 2012; Turner et al. 2012; Siidra et al. 2013; Kampf et al. 2013; Yang et al. 2013; Pinch et al. 2013). These minerals possess unusual and unique structures due to the adaptation of topology and geometry of silicate (or aluminosilicate) anions to the arrangements of the Pb^{2+} cations possessing stereochemically active $6s^2$ lone electron pairs. For

instance, the structures of maricopaite, $Ca_2Pb_7(Si_{36}Al_{12})O_{99}{\cdot}n(H_2O,OH)$ (Rouse and Peacor 1994) and rongibbsite, $[Pb_2OH][(Si_4Al)O_{11}]$ (Yang et al. 2013), contain interrupted tetrahedral frameworks with interruptions induced by the interaction of silicate species with polynuclear Pb-OH clusters present as complex extraframework cations. The structures of britvinite, $[Pb_7(OH)_3F(BO_3)_2(CO_3)][Mg_{4.5}(OH)_3(Si_5O_{14})]$ (Yakubovich et al. 2008) and molybdophyllite, $(Pb_4O)_2Mg_9[Si_{10}O_{28}](OH)_8(CO_3)_3{\cdot}H_2O$ (Kolitsch et al. 2012) possess complex $[Si_5O_{14}]$ tetrahedral sheets that can be viewed as interrupted mica-like silicate sheets. Stereochemical activity of lone electron pairs on Pb^{2+} cations seems to have a profound influence upon the structural features of silicate anions. The structure emerges as a result of a synergy between electronic and bonding requirements of the Pb^{2+} cations and flexibility of silicate tetrahedral units. The best way to understand this synergy is to investigate structures of 'pure' Pb silicates in the PbO-SiO_2 system, containing no additional cations and anions. However, only few data on these phases are available in the current literature. The only 'pure' Pb silicate mineral, alamosite, $PbSiO_3$ (Boucher and Peacor 1968; Krivovichev and Burns 2004), contains unusually distorted single silicate chain with 12 tetrahedra within its identity period (Liebau 1985). Other phases known in the PbO-SiO_2 system are synthetic Pb_2SiO_4 (= $Pb_2O[SiO_3]$) (Kato 1980; Dent Glasser et al. 1981), $Pb_3Si_2O_7$ (Petter et al. 1971), and $Pb_{11}Si_3O_{17}$ (= $Pb_{11}O_6[SiO_4][Si_2O_7]$) (Kato 1982). Herein we report on the synthesis and structural investigation of another synthetic Pb silicate, $Pb_7Si_6O_{19}$ (= $Pb_{21}[Si_7O_{22}]_2[Si_4O_{13}]$), and discuss its relations to hyttsjöite, $Pb_{18}Ba_2Ca_5Mn^{2+}{}_2Fe^{3+}{}_2Si_{30}O_{90}Cl{\cdot}6H_2O$ (Grew et al. 1996), a rare mineral from the Långban mines, Sweden.

Experimental

Crystals of the title compound have been prepared by crystallization from melt. The mixture of PbO (0.595 g, Aldrich, 99.95%) and SiO_2 (0.040 g, Aldrich, 99.98%) was placed into a platinum crucible on the substrate of $PbCl_2$ (2.000 g, Aldrich, 98%) used as a flux. The loaded crucible was heated to 920°C at the rate of 10°C/min and kept at this temperature for 30 min. Then it was cooled to

79 700°C at the cooling rate of 3°C/min and kept for 30 min, followed by cooling to room temperature at
80 the rate of 2°C/min. The product consisted of perfect hexagonal crystals of $Pb_{21}[Si_7O_{22}]_2[Si_4O_{13}]$
81 (Figure 1) grown on the bottom of crucible.
82 Qualitative analysis performed using the Hitachi TM 3000 electron microscope indicated the
83 absence of other elements with atomic number greater than 11 (Na), except Pb^{2+} and Si^{4+}.
84 One of the crystals obtained was crashed and suitable grain was mounted on a thin glass fiber
85 for the X-ray diffraction analysis. More than a hemisphere of X-ray diffraction data with frame widths
86 of 0.3º in ω, and 10 s spent counting for each frame were collected at room temperature using a Bruker
87 three-circle Smart APEX II X-ray diffractometer operated at 50 kV and 40 mA with MoKα radiation.
88 The data were integrated and corrected for absorption using an empirical ellipsoidal model by means of
89 the Bruker programs *APEX* and *XPREP*. The observed systematic absences were consistent with the
90 space group *P*-3. The structure was solved by direct methods and refined to $R_1 = 0.061$ on the basis of
91 F^2 for all unique data. The obtained structure model was transformed to the space group $P6_3/m$ using
92 the ADDSYM algorithm incorporated in the *PLATON* program package (Le Page, 1988; Speck, 2003).
93 Structure refinement in this group resulted in the crystallographic agreement index $R_1 = 0.042$ (Table
94 1). The *SHELX* program package was used for all structure calculations (Sheldrick, 2008). Positional
95 disorder was observed for one of the Pb sites, which appears to be splitted into three sites, Pb6, Pb6A
96 and Pb6A' (note that the Pb6A and Pb6A' sites are symmetrically equivalent), with a total occupancy
97 factor of 1. This kind of disorder for the Pb sites is typical for Pb silicates and aluminosilicates (see
98 Yang et al. (2013) and references therein). The final model included anisotropic displacement
99 parameters for all atoms. The final atomic coordinates and anisotropic displacement parameters are
100 given in Table 2 and selected interatomic distances in Table 3.
101
102 **Results**
103
104 **Silicate anions**

The structure of the title compound contains five symmetrically independent Si sites tetrahedrally coordinated by O atoms. The $Si1O_4$, $Si3O_4$ and $Si4O_4$ tetrahedra share corners to form branched heptameric $[Si_7O_{22}]^{16-}$ unit shown in Figure 2a. The unit has a shape of a tripod with the $Si4O_4$ tetrahedron at the top and $Si3O_4$ tetrahedra at the basis. Structural units of the same topology and very similar geometry have been observed previously in hyttsjöite (Grew et al. 1996). The $Si2O_4$ and $Si5O_4$ tetrahedra form the tetrameric $[Si_4O_{13}]^{10-}$ anion shown in Figure 2b. Note that the Si5 site is half-occupied, which corresponds to the orientation of the $Si5O_4$ tetrahedron either up or down relative to the plane of the unit. The $[Si_4O_{13}]^{10-}$ anions of the type shown in Figure 2b have not been observed in minerals, but were described in the structure of synthetic $NaBa_3Nd_3[Si_2O_7][Si_4O_{13}]$ (Malinovskii et al. 1983; Pushcharovsky, 1986).

Pb coordination

The structure contains six symmetrically independent Pb sites (Figure 3). The Pb6 and Pb6A sites have the site occupation factors (SOFs) of 1/3. The coordinations of the Pb atoms demonstrate very different degree of distortion. In general, there are three Pb-O bonds shorter than 2.6 Å that form PbO_3 trigonal pyramid with Pb at its apex. The PbO_3 configuration is complemented by five or six Pb-O bonds in the range of 2.6-3.5 Å. The coordination environments of the Pb6 and Pb6A sites are rather irregular, obviously, due to their low occupancies. The relative distortion of the PbO_n coordination polyhedra is due to the stereochemical activity of the lone electron pairs, which explains large variations in the Pb-O bond lengths within the same polyhedron.

Bond-valence analysis

Bond-valence calculations were performed using bond-valence parameters taken from Krivovichev and Brown (2001) for the Pb-O bonds and from Brown and Altermatt (1985) for the Si-O bonds. The results are presented in Table 4. As can be seen, there is a general agreement between the expected and calculated oxidation states for all atomic sites, except those that are either low-occupied

(Pb6, Pb6A, Si5, and O12) or bonded to the low-occupied sites (e.g., O11). Since bond-valence parameters are derived from the data obtained for fully ordered structures, there is still no accepted procedure in dealing with the bond-valence sums for the low-occupied sites, which usually essentialy deviate from the expected values.

Structure description

The structure of $Pb_{21}[Si_7O_{22}]_2[Si_4O_{13}]$ is shown in Figure 4a. It can be described as a stacking of layers of the two types, A and B. The A-type layer (Figure 4b) contains $[Si_7O_{22}]^{16-}$ units, Pb1, Pb2, Pb3, and Pb4 sites, whereas the B-type layer (Figure 4c) contains $[Si_4O_{13}]^{10-}$ anions, together with Pb5, Pb6, and Pb6A sites. The disorder observed for the Pb6 and Pb6A sites correlates with disordered orientation of the $Si5O_4$ tetrahedron (see above). The tripod-shaped $[Si_7O_{22}]^{16-}$ units have the same orientation within one A layer.

Stacking of the layers can be described as...AA'BAA'B..., where A and A' denote A layers with opposite orientations of the tripod-shaped silicate heptamers.

Discussion

Relations to hyttsjöite

The crystal structure of $Pb_{21}[Si_7O_{22}]_2[Si_4O_{13}]$ has many similarities to that of hyttsjöite, $Pb_{18}Ba_2Ca_5Mn^{2+}{}_2Fe^{3+}{}_2Si_{30}O_{90}Cl\cdot 6H_2O$ (Grew et al. 1996) = $Pb_{18}Ba_2Ca_5Mn^{2+}{}_2Fe^{3+}{}_2[Si_7O_{22}]_2[Si_8O_{23}]_2Cl\cdot 6H_2O$. As described by Grew et al. (1996), the latter consists of two types of plumbosilicate layers, L1 and L2. The L1 layers contain continuous $[Si_8O_{23}]^{14-}$ silicate sheets and Pb^{2+} cations. The L2 layers are virtually identical to the A sheets in the structure of $Pb_{21}[Si_7O_{22}]_2[Si_4O_{13}]$. The layers are based upon the same type of tripod-shaped silicate heptamers, $[Si_7O_{22}]^{16-}$. The stacking sequence of the layers in hyttsjöite can be described as ...L1 L1' L2 L2' L1 L1' L2 L2'..., where ' is used to identify opposite orientation of the sheets.

The most interesting common aspects of the structures of $Pb_{21}[Si_7O_{22}]_2[Si_4O_{13}]$ and hyttsjöite are the arrangements of tripod-shaped silicate heptamers in the adjacent plumbosilicate layers. They are stacked together in such a way that ellipsoidal cavities with dimensions of ca. 10×6×6 $Å^3$ are created. The cavity in hyttsjöite (Figure 5c) is occupied by the $ClPb_6$ octahedron (Figure 5d), i.e. the octahedron formed by six Pb atoms and centered by Cl. In contrast, in $Pb_{21}[Si_7O_{22}]_2[Si_4O_{13}]$, there is no Cl in the center of the cavity (Figure 5a), yielding an 'empty' $\square Pb_6$ octahedron (Figure 5b). Figure 5 shows that the size of the Pb_6 octahedra are approximately the same in the two structures, except in hyttsjöite it is larger, which can be explained by the large size of the Cl^- anion. The structural similarity of the double {L2L2'} and {AA'} layers in hyttsjöite and the title compound, respectively, is striking and may be interpreted as follows. The octahedral Pb_6 cavity in $Pb_{21}[Si_7O_{22}]_2[Si_4O_{13}]$ is occupied by the stereoactive lone electron pairs of the Pb^{2+} cations, which tend to associate into specific regions of the structure called lone-pair micelles (Makovicky 1997; Krivovichev et al. 2004; Siidra et al. 2009, 2010) or lone-pair self-containments (Johnston and Harrison 2002). The probable explanation for this effect is the electrophilicity of lone electron pairs that can be understood in terms of the hard-soft acid-base (HSAB) concept (Pearson 1988). The lone electron pairs on the cations behave as soft ligands that tend to associate together in a 'hard' environment. Therefore, the octahedral lone-pair micelles in $Pb_{21}[Si_7O_{22}]_2[Si_4O_{13}]$ with partially delocalized electron density are replaced by highly polarizable and soft Cl- anions in hyttsjöite. Very similar phenomenon has been observed by Frit et al. (1983) for two compounds, $Tl^{3+}{}_6O_6(TeO_6)$ and $Tl^{+}{}_6(TeO_6)$, which are isotypic, except for one symmetrically independent O site, which is present in the former and absent in the latter. In the structure of $Tl^{3+}{}_6O_6(TeO_6)$, this O atom occupies $[Tl_4]$ tetrahedron formed by four Tl^{3+} cations, whereas, in $Tl^{+}{}_6(TeO_6)$, the corresponding tetrahedron is empty.

According to Grew et al. (1996), hyttsjöite forms at temperatures near 500-600 °C and pressures 2-4 kbar. Similar conditions may also be suitable for the formation of $Pb_{21}[Si_7O_{22}]_2[Si_4O_{13}]$. Although no traces of Cl were observed by electron microprobe or single-crystal structure analysis, it seems possible that the presence of chlorine in the synthesis mixture may be necessary for the crystallization

of the title phase. One may speculate that tripod-shaped silicate heptamers with $ClPb_6$ octahedra at the center serve as prenucleation building blocks with subsequent removal of Cl.

Chemical and structural complexity of crystalline phases in the PbO-SiO_2 system

At the time of writing, there are four known structurally characterized crystalline phases in the PbO-SiO_2 system, and the title compound is the fifth. Crystallographic data for these compounds are given in Table 5, which also provides quantitative characteristics of their structural and chemical complexity calculated as follows.

The structural complexity is evaluated as an amount of structural information per atom (I_G) and per unit cell (u.c., $I_{G,total}$) according to the formulas (Krivovichev, 2012, 2013a, b):

$$I_G = -\sum_{i=1}^{k} p_i \log_2 p_i \qquad \text{(bits/atom)} \qquad (1),$$

$$I_{G,total} = -v\, I_G = -v \sum_{i=1}^{k} p_i \log_2 p_i \qquad \text{(bits/u.c.)} \qquad (2),$$

where k is the number of different crystallographic orbits and p_i is the random choice probability for an atom from the ith crystallographic orbit, that is:

$$p_i = m_i / v \qquad (3),$$

where m_i is a multiplicity of a crystallographic orbit relative to the reduced unit cell, and v is the number of atoms in the reduced unit cell.

The chemical complexity is estimated by considering chemical formula as a message, where symbols correspond to different chemical elements. For instance, Pb_2SiO_4 should be considered as PbPbSiOOOO, i.e. as a message of seven symbols that can be separated into three equivalence classes, {Pb}, {Si}, {O}, containing two, one, and four symbols, respectively. The amount of chemical information per formula then can be calculated as

$$^{chem}I = -n \sum_{i=1}^{k} p'_i \log_2 p'_i \qquad \text{(bits/formula)} \qquad (4),$$

where n is the number of atoms in the chemical formula, k is the number of different elements (= the number of equivalence classes), and is the random choice probability for an atom from the ith class:

$$p'_i = q_i / n \qquad (5),$$

where q_i is the number of atoms in the ith equivalence class.

For Pb_2SiO_4, $q_1\{Pb\} = 2$, $q_2\{Si\} = 1$, $q_3\{O\} = 4$, $n = 7$, which results in: $p'_1 = 2/7$, $p'_2 = 1/7$, $p'_3 = 4/7$. Therefore, ${}^{chem}I = -2\log_2(2/7) - \log_2(1/7) - 4\log_2(4/7) = 9.651$ bits/f.u. (f.u. = formula unit).

As can be seen from the data given in Table 5, there is a general trend of increasing structural information with the increasing chemical complexity. The most chemically complex phases appear to be the most complex from the structural point of view as well. The title phase appears to be the most structurally and chemically complex phase in the PbO-SiO_2 system known so far.

In general, structural organization of crystalline phases in the system can be described as follows. For the phases with Pb:Si < 2, their structures contain Pb^{2+} ions and silicate anions. The topological diversity of the silicate anions is controlled via the chemical complexity, i.e. complexity of the chemical formula. For the phases with Pb:Si ≥ 2, the structures contain 'additional' O atoms, i.e. atoms that are not bonded to Si. These atoms form strong bonds to the Pb atoms, which results in the formation of cationic OPb_4 tetrahedra, which are the next strongest structural subunits in the structure after silicate anions. Therefore the structure is considered as based upon silicate anions and polynuclear cationic units consisting of edge- and corner-sharing OPb_4 tetrahedra (Krivovichev and Filatov 1999; Siidra et al. 2008; Krivovichev et al. 2013). For instance, the structure of $Pb_2O[SiO_3]$ (Dent Glasser et al. 1981) contains $[Si_4O_{12}]^{8-}$ rings of SiO_4 tetrahedra and $[OPb_2]^{2+}$ chains of OPb_4 tetrahedra. More details on structural systematics of anion-centered tetrahedra and their occurence in minerals and inorganic compounds can be found in the recent review (Krivovichev et al. 2013).

Implications

In this study, using the example of the title compound, we demonstrated how structural complexity of lead silicates emerges as a result of interplay between stereochemical behaviour of lone electron pairs on Pb^{2+} cations and flexibility of tetrahedral silicate anions. In particular, comparison of the structure of $Pb_{21}[Si_7O_{22}]_2[Si_4O_{13}]$ with that of hyttsjöite shows that structural complexity of the latter is indeed induced by the electronic properties of Pb atoms rather than by general complex chemical composition. This kind of behaviour is observed in other natural Pb silicates as well, where lone electron pair stereoactivity induces either high periodicity of silicate chains (as in alamosite) or formation of interrupted tetrahedral frameworks (as in maricopaite and rongibbsite).

Acknowledgements

We are grateful to Anthony Kampf and an anonymous referee for useful remarks and suggestions. This work was supported by the Russian Federal Grant-in-Aid Program «Cadres» (agreement no. 8313) and RFBR research grant (# 12-05-31349). Technical support by the SPbSU X-Ray Diffraction Resource Center is gratefully acknowledged.

References

Belokoneva, E.L. and Dimitrova, O.V. (2011) Crystal structure $(Pb_{4.8}Na_{1.2})[Si_8(Si_{1.2}B_{0.8})O_{25}]$ with a new double tetrahedral layer and its comparison with hyttsjoeite, barisilite, benitoite, and langasite. Crystallography Reports, 56, 116-122.

Boucher, M.L. and Peacor, D.R. (1968) The crystal structure of alamosite, $PbSiO_3$. Zeitschrift für Kristallographie, 126, 98-111.

Brown, I.D. and Altermatt, D. (1985) Bond-valence parameters from a systematic analysis of the inorganic crystal structure database. Acta Crystallographica, B41, 244-247.

Chukanov, N.V., Yakubovich, O.V., Pekov, I.V., Belakovsky, D.I., and Massa, W. (2008) Britvinite,

$Pb_{15}Mg_9(Si_{10}O_{28})(BO_3)_4(CO_3)_2(OH)_{12}O_2$, a new mineral species from Långban, Sweden. Geology of Ore Deposits, 50, 713-719.

Dent Glasser, L.S., Howie, R.A., and Smart, R.M. (1981) The structure of lead 'orthosilicate', $(PbO)_2SiO_2$. Acta Crystallographica, B37, 303-306.

Frit, B., Roult, G., and Galy, J. (1983) Cristallochimie de $Tl(III)_6Te(VI)O_{12}$ et $Tl(I)_6Te(VI)O_6E_6$: un exemple original de l'activite stereochimique de la paire electronique $6s^2(E)$ du thallium(I). Journal of Solid State Chemistry, 48, 246-255.

Grew, E.S., Peacor, D.R., Rouse, R.C., Yates, M.G., Su, S.-C., and Marquez, N. (1996) Hyttsjoeite, a new, complex layered plumbosilicate with unique tetrahedral sheets from Langban, Sweden. American Mineralogist, 81, 743-753.

Johnston, M.G. and Harrison, W.T.A. (2002) Lone-pair self-containment in tellurite tubes: hydrothermal syntheses and structures of $BaTeO_7$ and $BaTe_4O_9$. Journal of the American Chemical Society, 124, 4576-4577.

Kampf, A.R., Rossman, G.R., and Housley, R.M. (2009) Plumbophyllite, a new species from the Blue Bell claims near Baker, San Bernardino County, California. American Mineralogist, 94, 1198–1204.

Kampf, A.R., Pluth, J.J., Chen, Y.-S., Roberts, A.C., and Housley, R.M. (2013) Bobmeyerite, a new mineral from Tiger, Arizona, USA, structurally related to cerchiaraite and ashburtonite. Mineralogical Magazine, 77, 81-91.

Kato, K. (1980) Die OD-Struktur von Bleisilicat Pb_2SiO_4 und Bleisilicat-Germanat-Mischkristall $Pb_2(SiGe)O_4$. Acta Crystallographica, B36, 2539-2545.

Kato, K. (1982) Die Kristallstruktur des Bleisilicats $Pb_{11}Si_3O_{17}$. Acta Crystallographica, B38, 57-62.

Kolitsch, U., Merlino, S., and Holtstam, D. (2012) Molybdophyllite: crystal chemistry, crystal structure, OD character and modular relationships with britvinite. Mineralogical Magazine, 76, 493-516.

283 Krivovichev, S.V (2012) Topological complexity of crystal structures: quantitative approach. Acta
284 Crystallographica, A68, 393-398.
285 Krivovichev, S.V. (2013a) Structural complexity of minerals: information storage and processing in the
286 mineral world. Mineralogical Magazine, 77, 275-326.
287 Krivovichev, S.V. (2013b) Which inorganic structures are the most complex? Angewandte Chemie
288 International Edition, accepted. DOI: 10.1002/anie.201304374.
289 Krivovichev, S.V. and Brown, I.D. (2001) Are the compressive effects of encapsulation an artefact of
290 the bond valence parameters? Zeitschrift für Kristallographie, 216, 245-247.
291 Krivovichev, S.V. and Burns, P.C. (2004) Crystal structure of synthetic alamosite $Pb(SiO_3)$. Zapiski
292 Vserossijskogo Mineralogicheskogo Obshchestva, 133(5), 70-76 (in Russian).
293 Krivovichev, S.V. and Filatov, S.K. (1999) Structural principles for minerals and inorganic compounds
294 containing anion-centered tetrahedra. American Mineralogist, 84, 1099-1106.
295 Krivovichev, S.V., Armbruster, T., and Depmeier, W. (2004) One-dimensional lone electron pair
296 micelles in the crystal structure of $Pb_5(SiO_4)(VO_4)_2$. Materials Research Bulletin, 39, 1717-1722.
297 Krivovichev, S.V., Mentré, O., Siidra, O.I., Colmont, M., and Filatov, S.K. (2013) Anion-centered
298 tetrahedra in inorganic compounds. Chemical Reviews, 113, 6459-6535.
299 Le Page, Y. (1988) MISSYM1.1 - a flexible new release. Journal of Applied Crystallography, 21, 983-
300 984.
301 Liebau, F. (1985) Structural Chemistry of Silicates. Structure, Bonding and Classification. Springer
302 Verlag, Berlin.
303 Makovicky, E. (1997) Modular and crystal chemistry of sulfosalts and other complex sulfides. In:
304 Merlino, S. (ed). Modular Aspects of Minerals. EMU Notes in Mineralogy, Vol. 1. Eotvos
305 Univesity Press, Budapest, pp. 237-271.
306 Malinovskii, Yu.A., Baturin, S.V., and Bondareva, O.S. (1983) A new island silicate radical $[Si_4O_{13}]$ in
307 the structure of $NaBa_3Nd_3[Si_2O_7][Si_4O_{13}]$. Soviet Physics Doklady 28, 809-812.
308 Pearson, R.G. (1988) Absolute electronegativity and hardness: application to inorganic chemistry.

Inorganic Chemistry, 27, 734-740.

Petter, W., Harnik, A.B., and Keppler, U. (1971) Die Kristallstruktur von Blei-Barysilit, $Pb_3Si_2O_7$. Zeitschrift für Kristallographie, 133, 445-458.

Pinch, W.W., Downs, R.T., Evans, S.H., Megaw, L., and Bloch, E.M. (2013) Yangite, IMA 2012-052. CNMNC Newsletter No. 15. Mineralogical Magazine, 77, 1-12.

Pushcharovsky, D.Yu. (1986) Structural Mineralogy of Silicates and Their Synthetic Analogs. Moscow Nedra (in Russian).

Rouse, R.C. and Peacor, D.R. (1994) Maricopaite, an unusual lead calcium zeolite with an interrupted mordenite-like framework and intrachannel Pb_4 tetrahedral clusters. American Mineralogist, 79, 175–184.

Sheldrick, G.M. (2008) A short history of *SHELX*. Acta Crystallographica, A64, 112–122.

Siidra, O.I., Krivovichev, S.V., and Filatov, S.K. (2008) Minerals and synthetic Pb(II) compounds with oxocentered tetrahedra: review and classification. Zeitschrift für Kristallographie, 223, 114-125.

Siidra, O.I., Britvin, S.N., and Krivovichev, S.V. (2009) Hydroxocentered $[(OH)Tl_3]^{2+}$ triangle as a building unit in thallium compounds: Synthesis and crystal structure of $Tl_4(OH)_2CO_3$. Zeitschrift für Kristallographie, 224, 563-567.

Siidra, O.I., Britvin, S.N., Krivovichev, S.V., and Depmeier, W. (2010) Polytypism of layered alkaline hydroxides: Crystal structure of TlOH. Zeitschrift für Anorganische und Allgemeine Chemie, 636, 595-599.

Siidra, O.I., Krivovichev, S.V., Turner, R.W., Rumsey, M.S., and Spratt, J. (2013) Crystal chemistry of layered Pb oxychloride minerals with PbO-related structures: Part I. Crystal structure of hereroite, $[Pb_{32}O_{20}(O,\square)](AsO_4)_2[(Si,As,V,Mo)O_4]_2Cl_{10}$. American Mineralogist, 98, 248-255.

Speck, A.L. (2003) Single-crystal structure validation with the program *PLATON*. Journal of Applied Crystallography, 36, 7-13.

Turner, R., Siidra, O.I., Rumsey, M.S., Krivovichev, S.V., Stanley, C.J., and Spratt, J. (2012) Hereroite and vladkrivovichevite: two novel lead oxychlorides from the Kombat mine, Namibia. Mineralogical Magazine, 76, 883-890.

Yakubovich, O.V., Massa, W., and Chukanov, N.V. (2008) Crystal structure of britvinite $[Pb_7(OH)_3F(BO_3)_2(CO_3)][Mg_{4.5}(OH)_3(Si_5O_{14})]$: a new layered silicate with an original type of silicon-oxygen networks. Crystallography Reports, 53, 206-215.

Yang, H., Downs, R.T., Evans, S.H., Jenkins, R.A., and Bloch, E.M. (2013) Rongibbsite, $Pb_2(Si_4Al)O_{11}(OH)$, a new zeolitic aluminosilicate mineral with an interrupted framework from Maricopa County, Arizona, U.S.A. American Mineralogist, 98, 236-241.

344 Figures

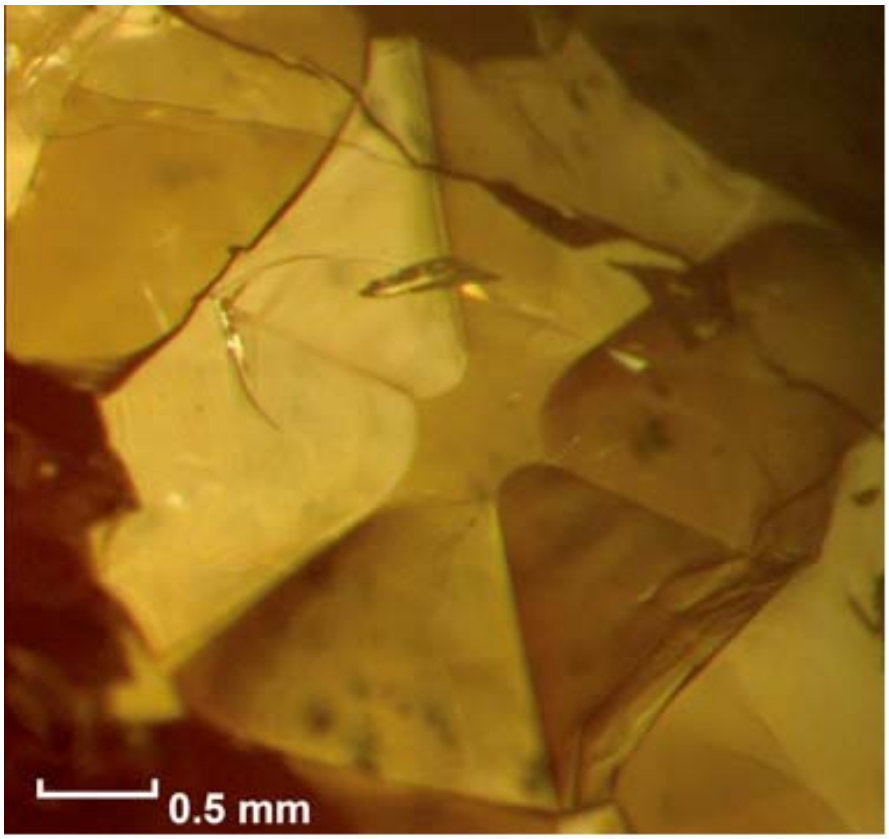

345

346 **Figure 1.** Yellow hexagonal crystals of $Pb_{21}[Si_7O_{22}]_2[Si_4O_{13}]$ under optical microscope.

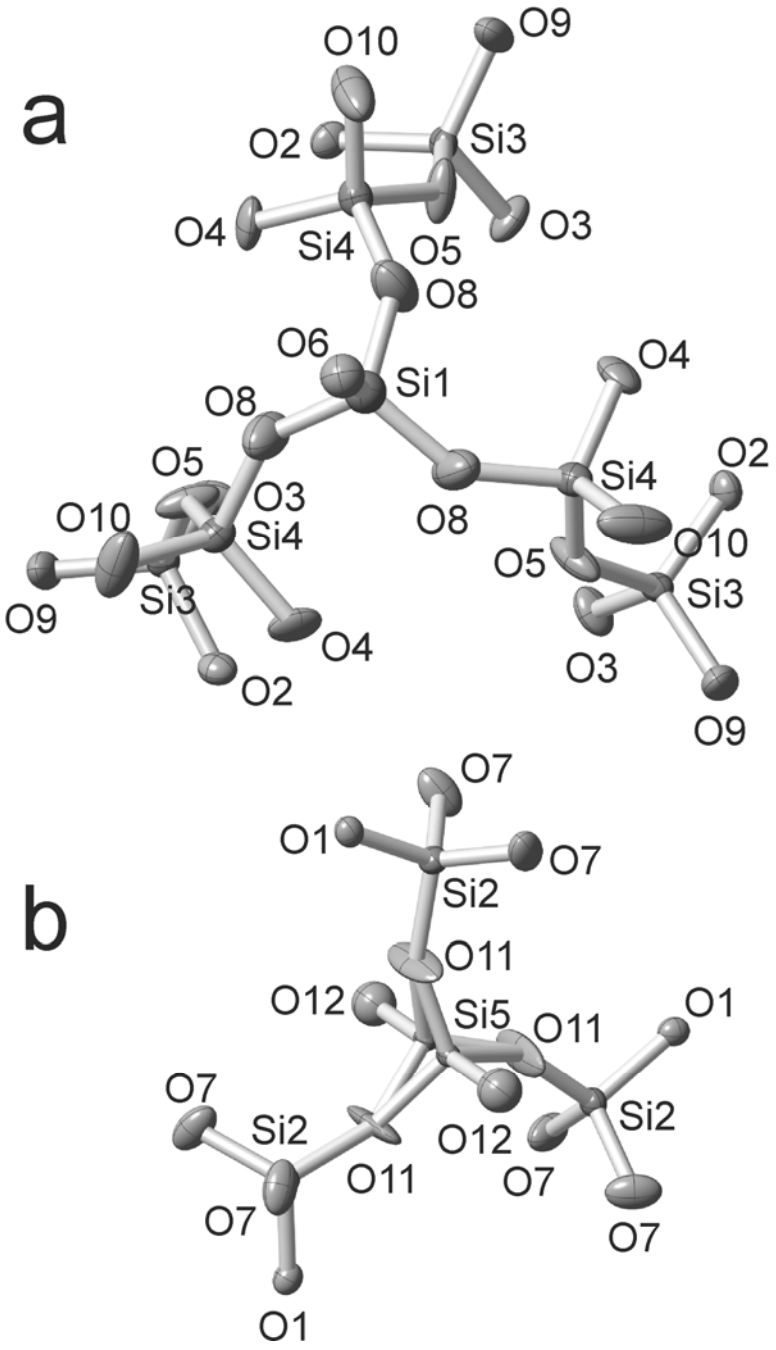

Figure 2. Silicate anions in the crystal structure of $Pb_{21}[Si_7O_{22}]_2[Si_4O_{13}]$.

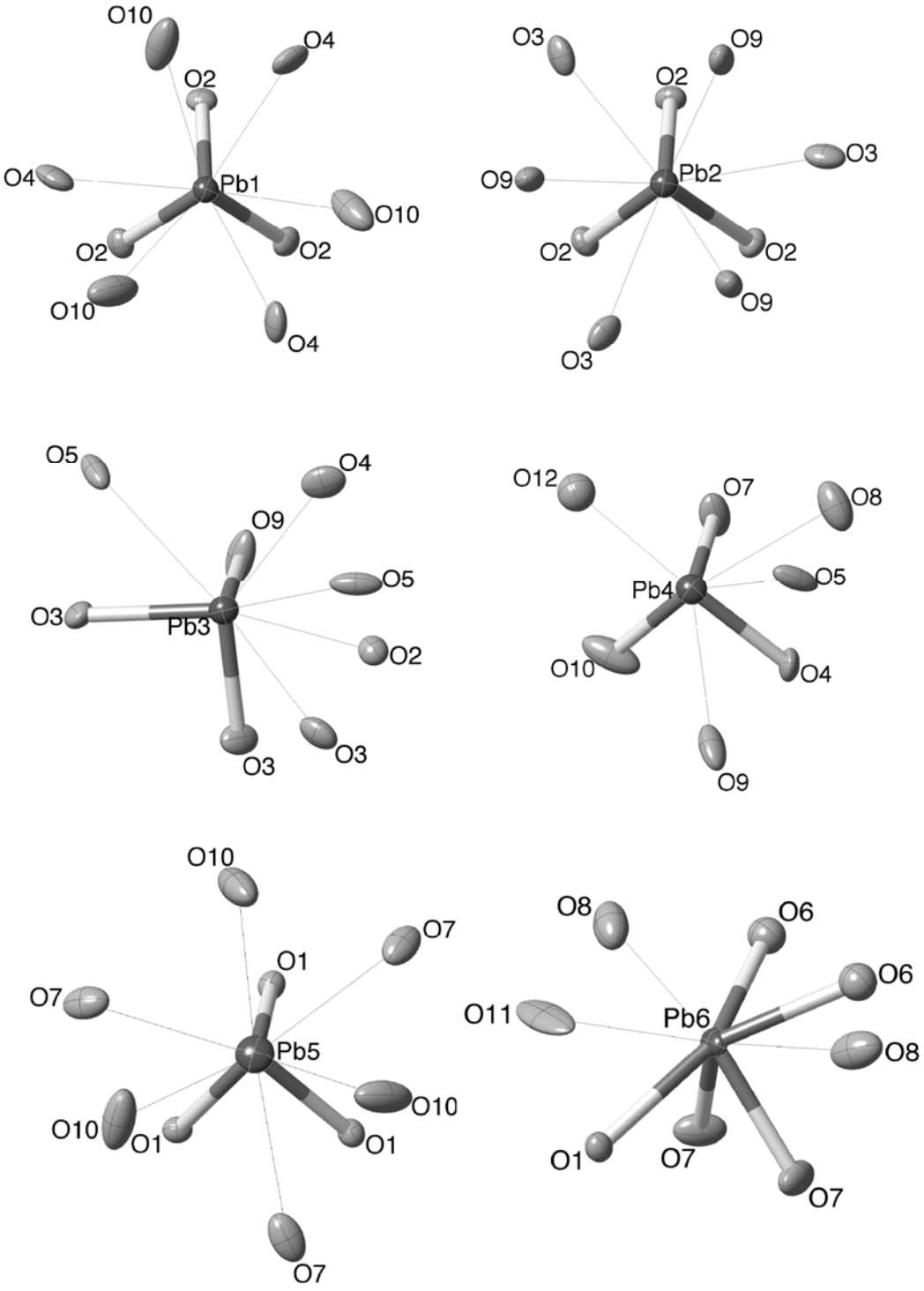

Figure 3. Coordination of Pb atoms in the crystal structure of $Pb_{21}[Si_7O_{22}]_2[Si_4O_{13}]$.

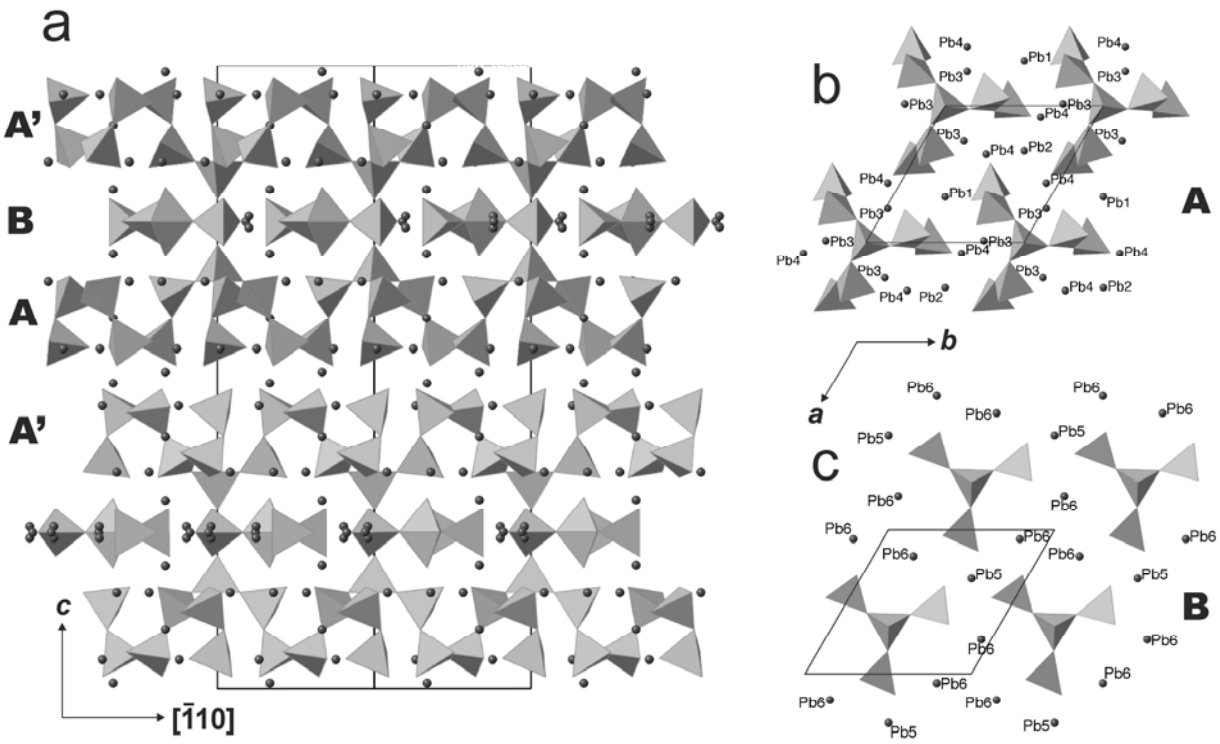

352

353

354 **Figure 4**. The crystal structure of $Pb_{21}[Si_7O_{22}]_2[Si_4O_{13}]$ projected along [110] (a) and projections of the

355 A and B layers onto the (001) plane (b).

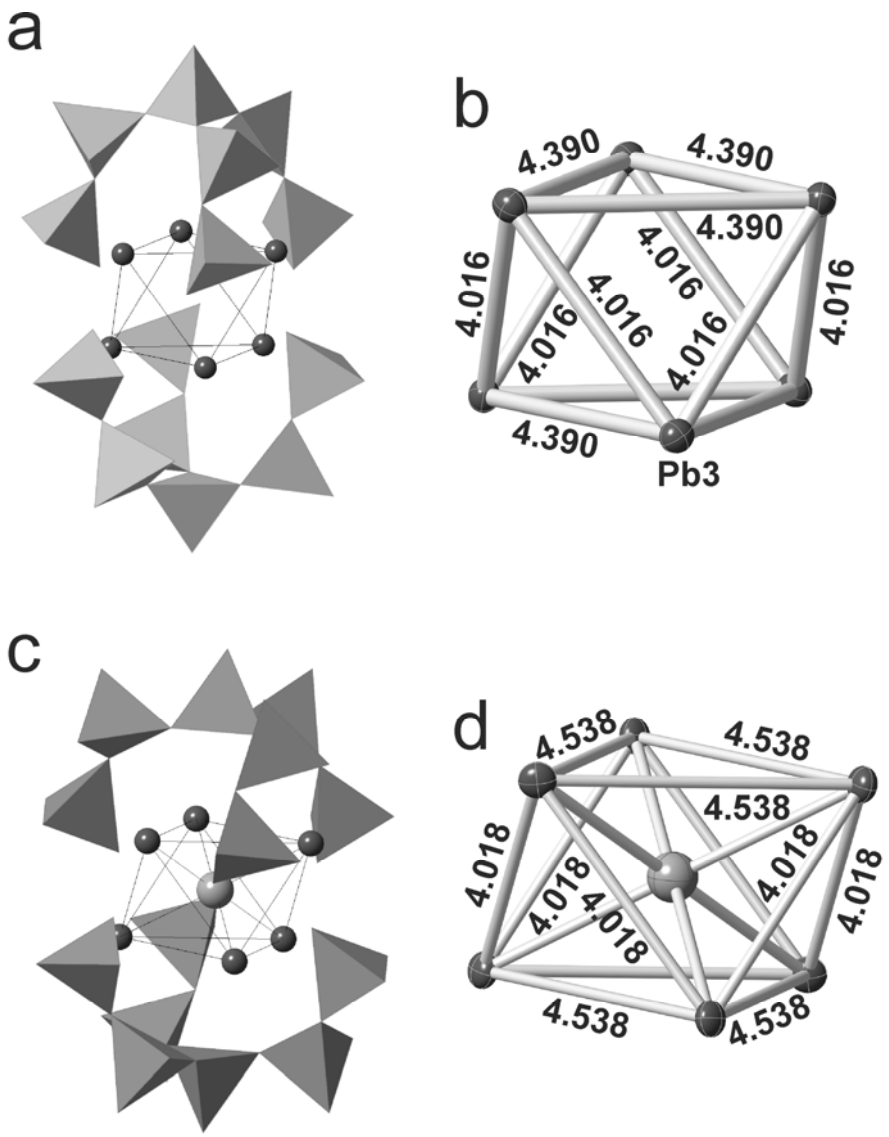

Figure 5. Ellipsoidal cavities formed by $[Si_7O_{22}]$ silicate anions in the crystal structures of $Pb_{21}[Si_7O_{22}]_2[Si_4O_{13}]$ (a) and hyttsjöite (c) are occupied by the $\square Pb_6$ (b) and $ClPb_6$ (d) octahedral clusters, respectively.

365 **Table 1.** Crystallographic data and refinement
366 parameters for $Pb_{21}[Si_7O_{22}]_2[Si_4O_{13}]$

Crystal size (mm^3)	0.14×0.15×0.09
Space group	$P6_3/m$
a (Å)	9.9244(5)
c (Å)	34.2357(16)
V ($Å^3$)	795.28(6)
μ (mm^{-1})	60.771
D_{calc} (g/cm^3)	6.560
Radiation wavelength (Å)	0.71073 (MoKα)
θ-range (deg.)	1.19-36.36
Total Ref.	28731
Unique Ref.	4625
Unique $\|Fo\| \geq 4s_F$	3361
R_{int}	0.08
R_1	0.042
R_1 (all data)	0.072
GoF	1.090
$\rho_{max,min}$ ($e \cdot Å^{-3}$)	+4.283/-3.306

367

368 **Table 2.** Atomic coordinates and displacement parameters (Å^2) for $Pb_{21}[Si_7O_{22}]_2[Si_4O_{13}]$

Atom	*x*	*y*	*z*	U_{eq}	U_{11}	U_{22}	U_{33}	U_{23}	U_{13}	U_{12}
Pb1	2/3	1/3	0.594983(16)	0.01184(10)	0.01273(14)	0.01273(14)	0.0101(2)	0	0	0.00637(7)
Pb2	2/3	1/3	0.490651(16)	0.01352(11)	0.01453(15)	0.01453(15)	0.0115(2)	0	0	0.00726(7)
Pb3	0.75175(4)	0.01367(4)	0.545490(10)	0.01375(7)	0.01206(13)	0.01489(14)	0.01423(13)	0.00059(12)	-0.0002(1)	0.00668(12)
Pb4	0.08035(4)	0.64380(4)	0.653630(10)	0.01664(7)	0.01375(14)	0.01605(15)	0.01811(15)	0.00081(12)	0.00214(12)	0.00594(12)
Pb5	2/3	1/3	0.698105(18)	0.02069(12)	0.02583(18)	0.02583(18)	0.0104(2)	0	0	0.01292(9)
Pb6*	0.8208(5)	0.7603(5)	¾	0.0122(6)	0.0061(7)	0.0120(9)	0.0181(15)	0	0	0.0042(7)
Pb6A*	0.8013(4)	0.7563(4)	0.74109(15)	0.0481(10)	0.0445(16)	0.0481(13)	0.066(3)	0.0258(15)	0.0321(16)	0.0335(12)
Si1	0	0	0.66788(15)	0.0206(9)	0.0195(13)	0.0195(13)	0.023(2)	0	0	0.0098(6)
Si2	0.9873(4)	0.5707(4)	¾	0.0118(6)	0.0093(14)	0.0103(14)	0.0145(15)	0	0	0.0040(12)
Si3	0.6029(3)	0.6077(3)	0.55296(7)	0.0101(4)	0.0115(10)	0.0108(10)	0.0090(9)	0.0005(8)	-0.0019(8)	0.0062(8)
Si4	0.9360(3)	0.2492(3)	0.63335(7)	0.0134(4)	0.0131(10)	0.0148(11)	0.0104(10)	0.0009(9)	0.0000(9)	0.0056(9)
Si5**	1/3	2/3	0.7398(2)	0.0085(14)	0.0071(17)	0.0071(17)	0.011(3)	0	0	0.0036(8)
O1	0.8553(10)	0.3855(10)	¾	0.0125(16)	0.015(4)	0.013(4)	0.010(4)	0	0	0.008(3)
O2	0.6955(7)	0.5135(7)	0.54715(18)	0.0137(11)	0.017(3)	0.012(3)	0.013(3)	-0.002(2)	0.001(2)	0.007(2)
O3	0.6446(8)	0.7344(8)	0.5187(2)	0.0191(13)	0.031(4)	0.017(3)	0.015(3)	0.005(3)	0.003(3)	0.016(3)
O4	0.7599(7)	0.1252(8)	0.6215(2)	0.0213(14)	0.009(3)	0.026(3)	0.024(4)	0.008(3)	0.005(3)	0.005(3)
O5	0.0389(7)	0.3315(9)	0.59424(19)	0.0224(15)	0.012(3)	0.033(4)	0.012(3)	0.011(3)	0.001(3)	0.003(3)
O6	0	0	0.7141(4)	0.022(2)	0.021(3)	0.021(3)	0.024(6)	0	0	0.0105(17)
O7	0.9638(9)	0.6542(8)	0.7121(2)	0.0245(15)	0.037(4)	0.028(4)	0.017(3)	0.009(3)	0.012(3)	0.023(3)
O8	0.1412(9)	0.9762(9)	0.6532(3)	0.0301(18)	0.026(4)	0.027(4)	0.042(5)	0.006(4)	0.016(4)	0.016(3)
O9	0.4174(8)	0.4943(8)	0.5569(3)	0.0284(18)	0.011(3)	0.014(3)	0.058(6)	-0.004(3)	-0.002(3)	0.005(3)
O10	0.9442(9)	0.3821(9)	0.6617(3)	0.037(2)	0.032(4)	0.021(4)	0.042(5)	-0.013(4)	0.016(4)	0.002(3)
O11	0.1581(11)	0.5831(12)	¾	0.048(4)	0.005(4)	0.015(5)	0.119(14)	0	0	0.001(4)
O12**	1/3	2/3	0.6943(8)	0.027(5)						

369 *SOF = 0.333. **SOF = 0.5.

370 **Table 3.** Selected interatomic distances in the structure of
371 $Pb_{21}[Si_7O_{22}]_2[Si_4O_{13}]$

Pb1-O2(×3)	2.334(6)	Pb6A-Pb6A	0.610(10)
Pb1-O4(×3)	2.804(7)	Pb6A-O6	2.413(6)
Pb1-O10(×3)	3.420(10)	Pb6A-O7	2.498(8)
		Pb6A-O1	2.518(9)
Pb2-O2(×3)	2.551(6)	Pb6A-O6	2.705(8)
Pb2-O9(×3)	2.775(8)	Pb6A-O7	2.797(8)
Pb2-O3(×3)	2.832(7)	Pb6A-O8	3.142(10)
		Pb6A-O10	3.304(11)
Pb3-O9	2.175(7)	Pb6A-O11	3.320(11)
Pb3-O3	2.359(7)		
Pb3-O3	2.589(7)	Si1-O6	1.584(14)
Pb3-O2	2.621(6)	Si1-O8(×3)	1.613(7)
Pb3-O4	2.814(8)		
Pb3-O5	3.193(7)	Si2-O7(×2)	1.617(7)
Pb3-O5	3.445(7)	Si2-O11	1.637(11)
Pb3-O9	3.496(7)	Si2-O1	1.639(9)
Pb4-O10	2.267(8)	Si3-O9	1.613(7)
Pb4-O4	2.279(6)	Si3-O3	1.614(7)
Pb4-O7	2.341(7)	Si3-O2	1.618(6)
Pb4-O12	2.780(14)	Si3-O5	1.660(7)
Pb4-O8	3.043(7)		
Pb4-O9	3.365(9)	Si4-O10	1.606(8)
Pb4-O5	3.443(7)	Si4-O4	1.606(7)
Pb4-O11	3.508(4)	Si4-O8	1.627(8)
		Si4-O5	1.634(7)
Pb5-O1(×3)	2.442(6)		
Pb5-O10(×3)	2.836(8)	Si5-Si5	0.697(15)
Pb5-O7(×3)	3.111(8)	Si5-O11(×3)	1.547(10)
		Si5-O12	1.56(3)
Pb6-Pb6A	0.353(4)	Si5-O12	2.25(3)
Pb6-O6(×2)	2.469(7)		
Pb6-O7(×2)	2.509(8)		
Pb6-O1	2.569(9)		
Pb6-O8(×2)	3.439(9)		
Pb6-O11	3.476(11)		

372

373 **Table 4.** Bond-valence analysis (v.u.) for the crystal structure of $Pb_{21}[Si_7O_{22}]_2[Si_4O_{13}]$

Atom	O1	O2	O3	O4	O5	O6	O7	O8	O9	O10	O11	O12*	Sum
Pb1		$0.47^{3\times\rightarrow}$		$0.18^{3\times\rightarrow}$						$0.05^{3\times\rightarrow}$			2.10
Pb2		$0.30^{3\times\rightarrow}$	$0.17^{3\times\rightarrow}$						$0.19^{3\times\rightarrow}$				1.98
Pb3		0.26	0.45+0.28	0.18	0.08+0.05				0.65+0.04				1.99
Pb4				0.53	0.05		0.46	0.11	0.06	0.54	$0.04^{2\times\downarrow}$	$0.19^{3\times\downarrow}$	1.98
Pb5	$0.38^{3\times\rightarrow 2\times\downarrow}$						$0.10^{3\times\rightarrow}$			$0.17^{3\times\rightarrow}$			1.95
Pb6**	0.29					$0.36^{2\times\rightarrow 3\times\downarrow}$	$0.33^{2\times\rightarrow}$	$0.05^{2\times\rightarrow}$			0.05		1.77
Pb6A**	0.32					$0.40+0.22^{3\times\downarrow}$	0.34+0.18	0.09		0.07	0.06		1.68
Si1						1.11		$1.03^{3\times\rightarrow}$					4.20
Si2	0.96						$1.02^{2\times\rightarrow}$				0.97		3.97
Si3		1.02	1.03		0.91				1.03				3.99
Si4				1.05	0.97			0.99		1.05			4.06
Si5*											$1.23^{3\times\rightarrow}$	1.19	4.88
Sum	2.03	2.05	1.93	1.94	2.06	2.13	2.17	2.23	1.97	1.88	2.39	1.76	

374 * SOF = 0.5. ** SOF = 0.333.
375

376 **Table 5.** Crystallographic data and complexity parameters for Pb silicates

Pb:Si	Chemical formula	Sp. gr.	*a* [Å] / *α* [deg]	*b* [Å] / *β* [deg]	*c* [Å] / *γ* [deg]	*v* [atoms]	I_G [bits/atom]	$I_{G,total}$ [bits/u.c.]	I_{chem} [bits/f.u.]	Ref.
1.000	$Pb[SiO_3]$	*P*2/*n*	11.209 / 90	7.0410 / 113.0	12.220 / 90	60	3.974	238.413	6.855	1
1.167	$Pb_{21}[Si_7O_{22}]_2[Si_4O_{13}]$	$P6_3/m$	9.924 / 90	9.924 / 90	34.236 / 120	194	4.361	846.109	44.128	2
1.500	$Pb_3[Si_2O_7]$	*R*-3*c*	10.126 / 90	10.1264 / 90	38.678 / 120	72	2.828	203.627	16.613	3
2.000	$Pb_2O[SiO_3]$	*A*121	19.43 / 90	7.64 / 99.33	12.24 / 90	56	4.879	273.212	9.651	4
3.667	$(Pb_2O)_2(Pb_7O_3)O[SiO_4][Si_2O_7]$	*P*-1	22.502 / 92.5	12.982 / 99.2	7.313 / 100.3	124	5.954	738.320	41.285	5

377 **References**: (1) Krivovichev and Burns 2004; (2) this work; (3) Petter et al. 1971; (4) Dent Glasser et al. 1981; (5) Kato 1982.
378

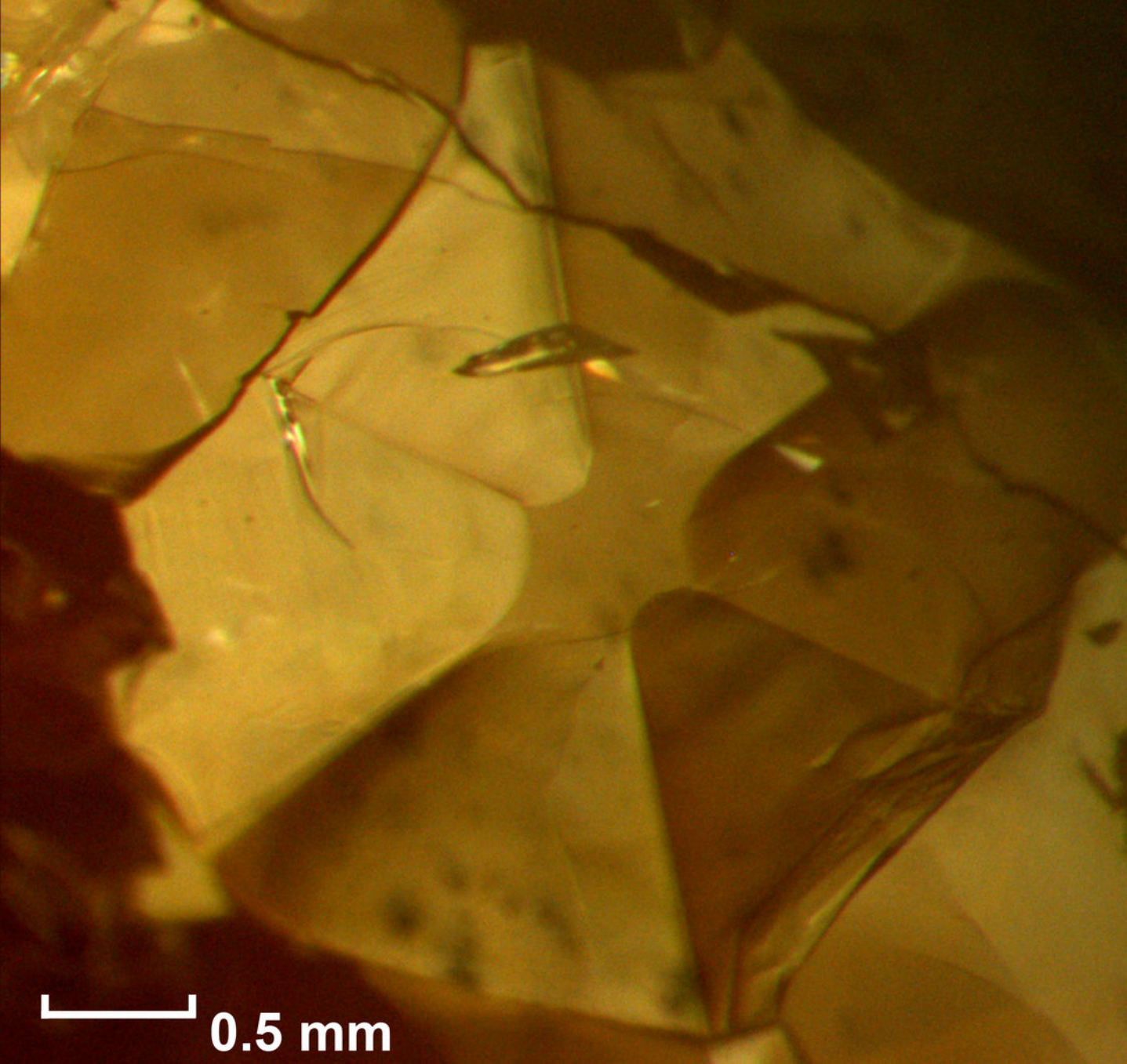
0.5 mm

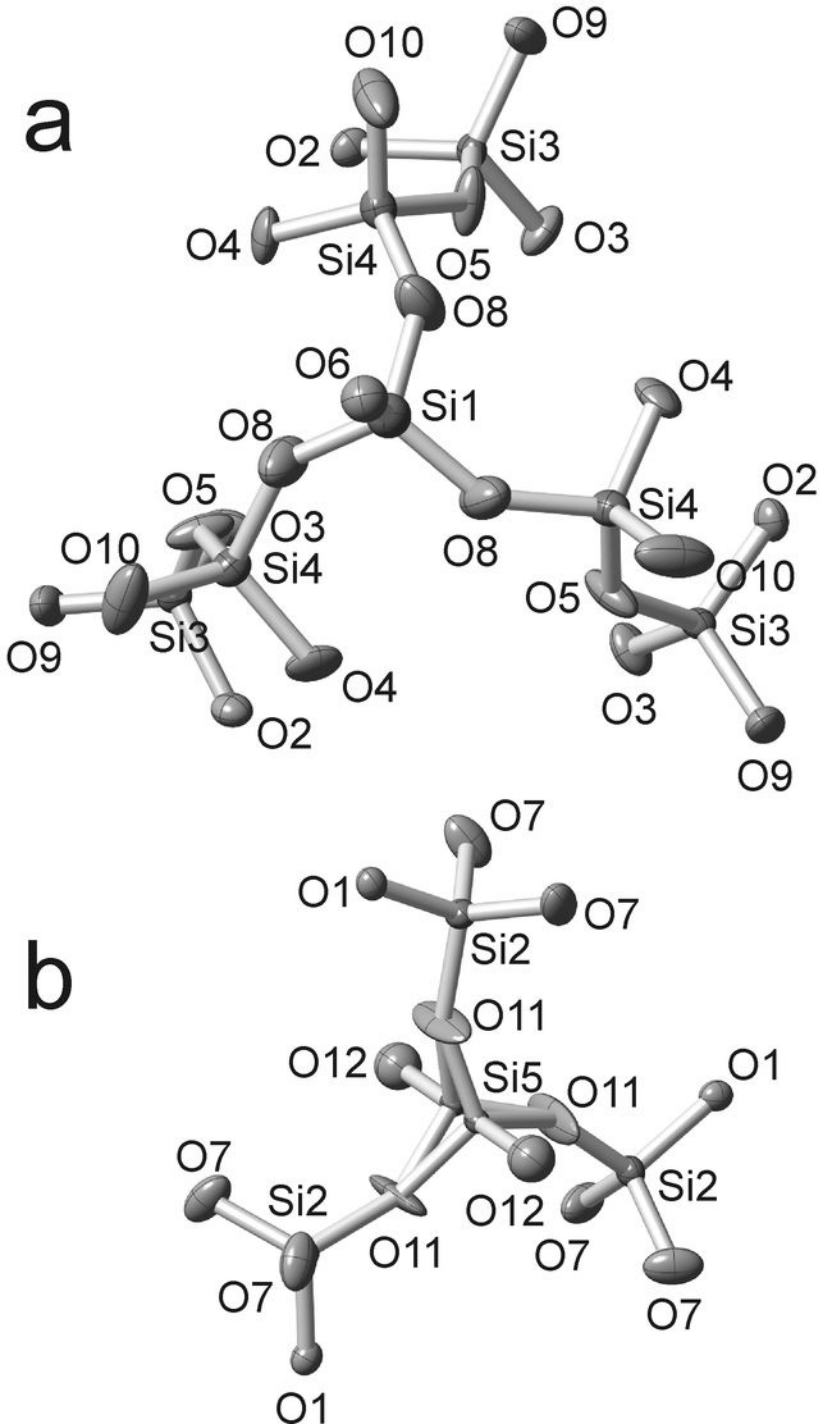
a
O10
O9
O2
Si3
O4
Si4
O5
O3
O8
O6
Si1
O4
O8
O5
O3
Si4
O2
O10
O8
O10
Si4
O5
Si3
O9
Si3
O4
O3
O2
O9
b
O7
O1
O7
Si2
O11
O12
Si5
O11
O1
O7
Si2
O12
Si2
O11
O7
O7
O7
O1

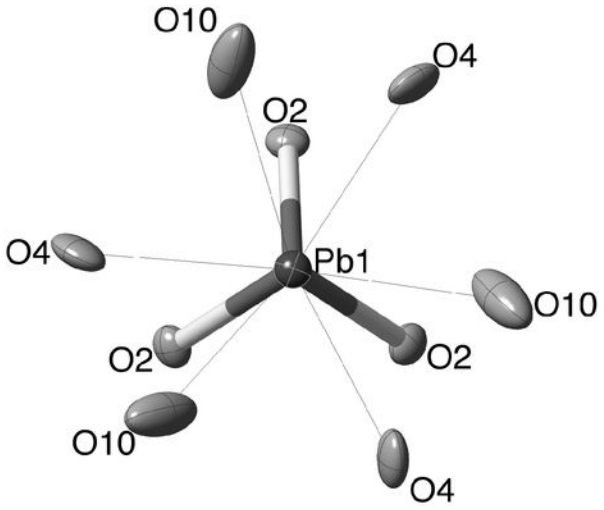
O10
O4
O2
O4
Pb1
O10
O2
O2
O10
O4

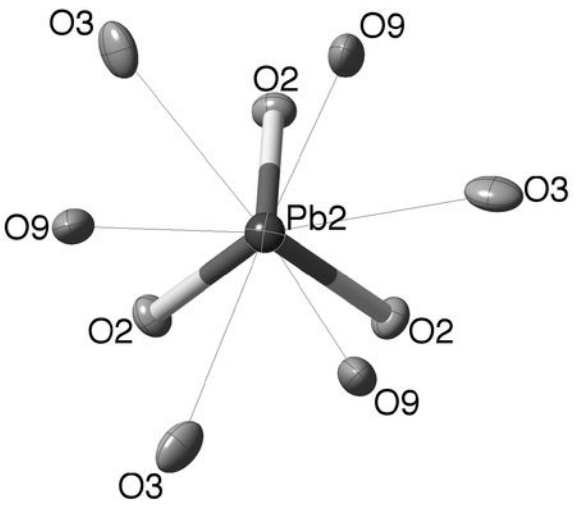
O3
O9
O2
O3
O9
Pb2
O2
O2
O9
O3

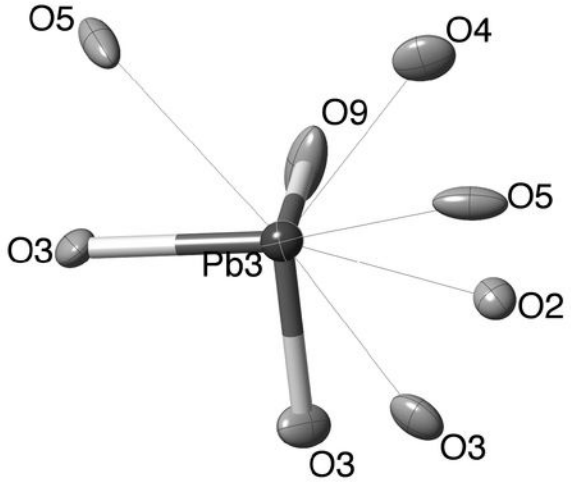
O5
O4
O9
O5
O3
Pb3
O2
O3
O3

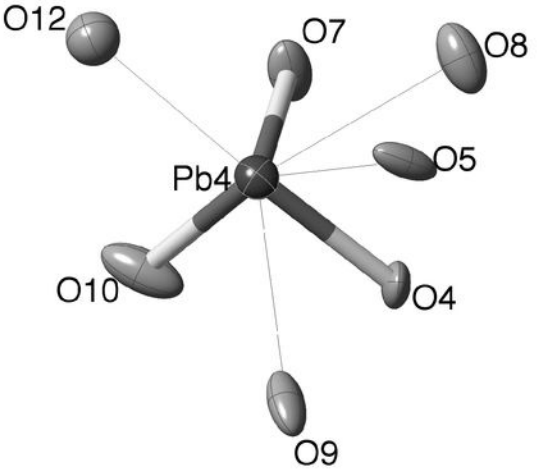
O12
O7
O8
O5
Pb4
O10
O4
O9

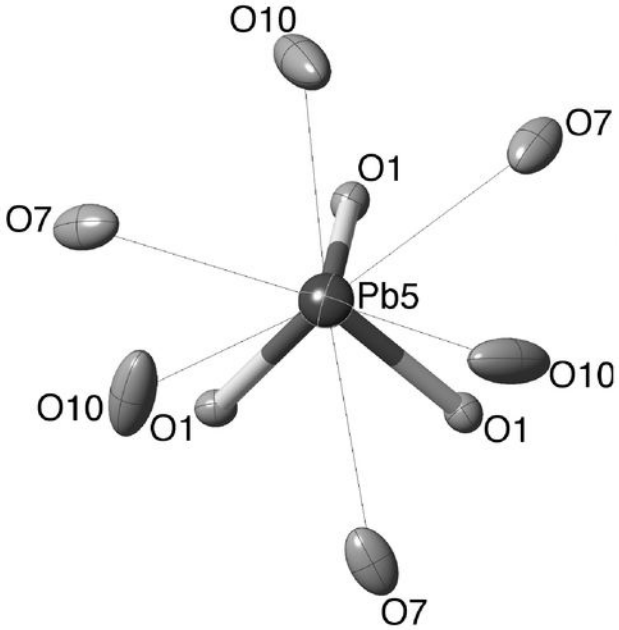
O10
O7
O1
O7
Pb5
O10
O10
O1
O1
O7

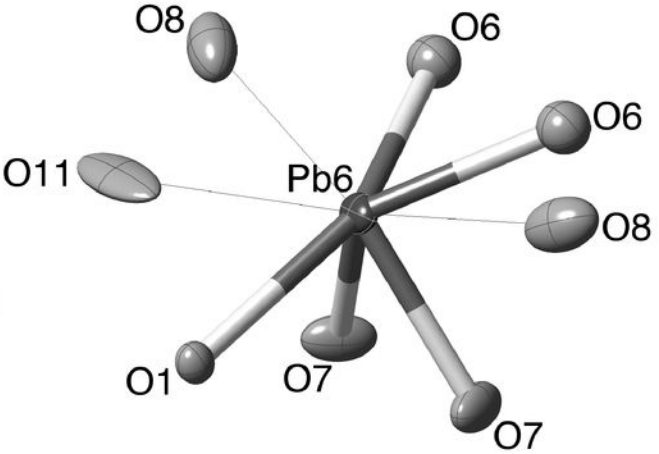
O8
O6
O6
O11
Pb6
O8
O1
O7
O7

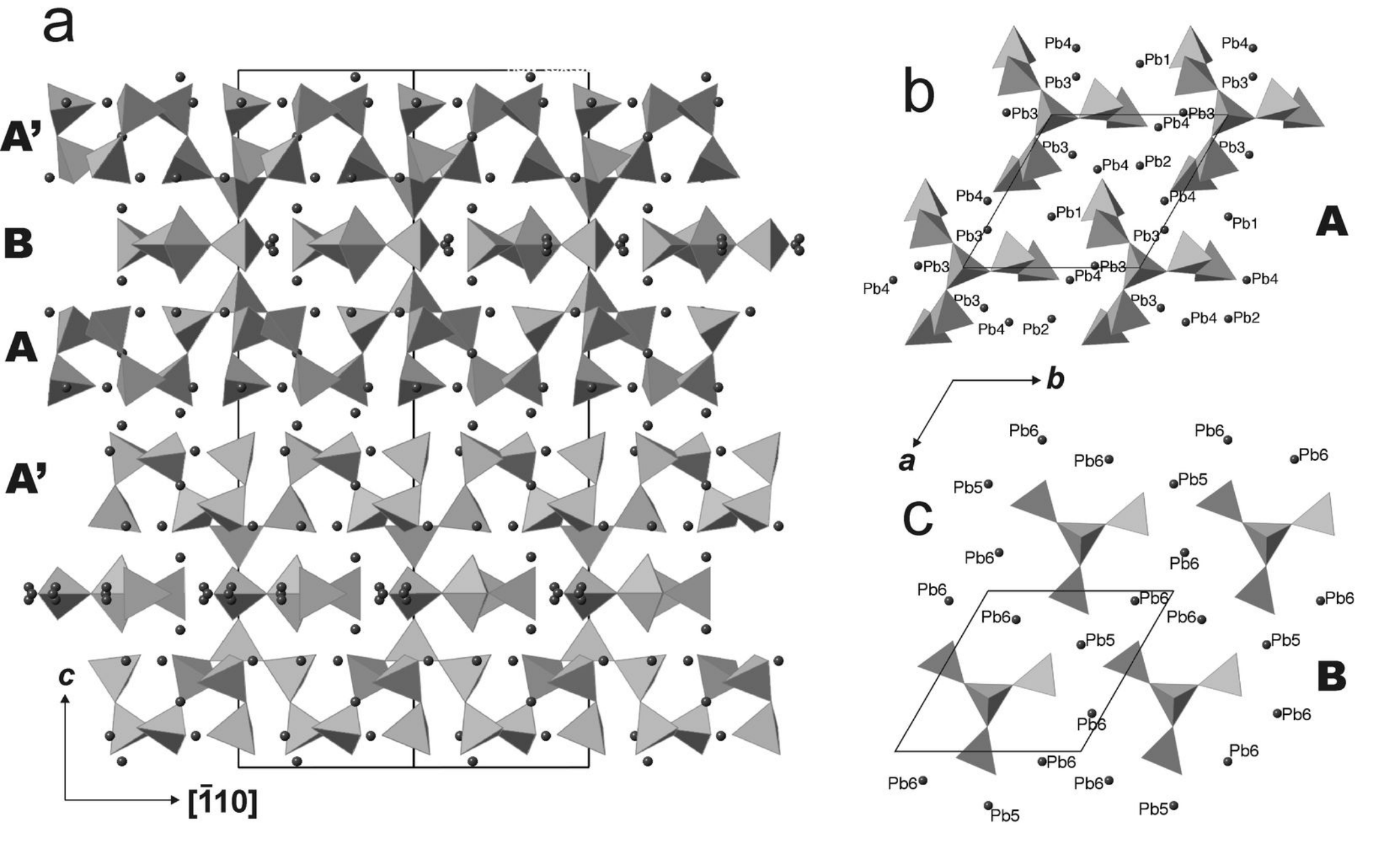
a
A'
B
A
A'
c
[$\bar{1}$10]
b
Pb4
Pb1
Pb3
Pb2
A
b
a
C
Pb6
Pb5
B

a

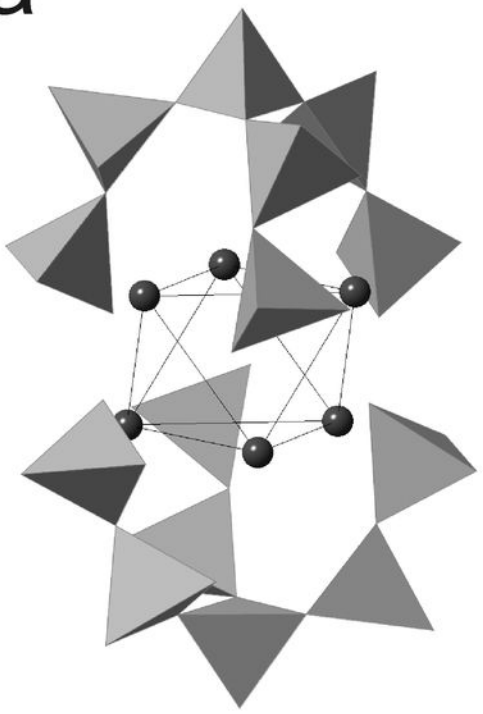

b

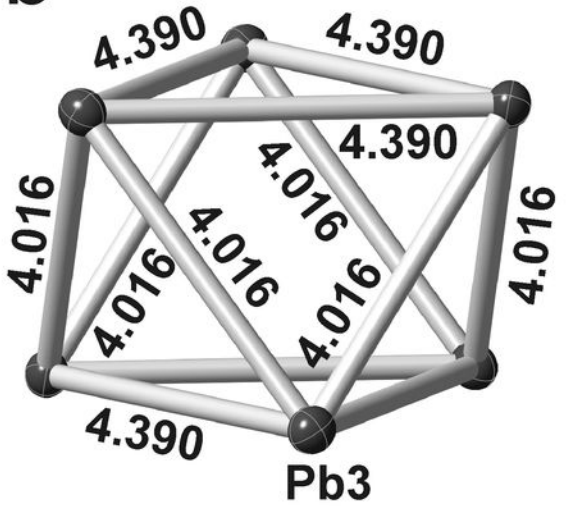
4.390
4.390
4.390
4.016
4.016
4.016
4.016
4.016
4.016
4.016
4.390
Pb3

c

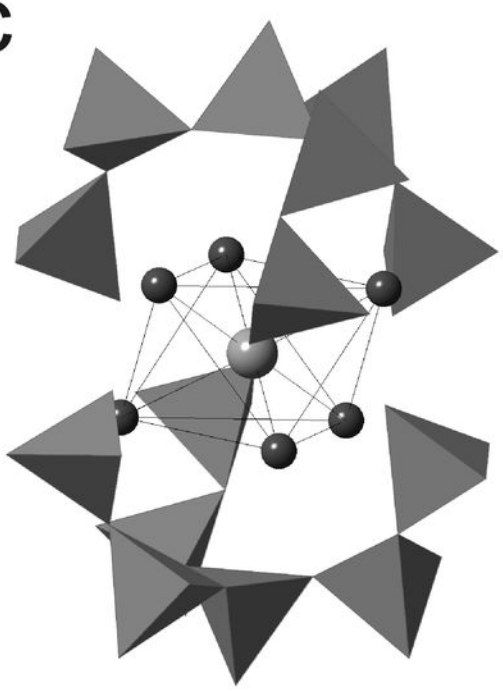

d

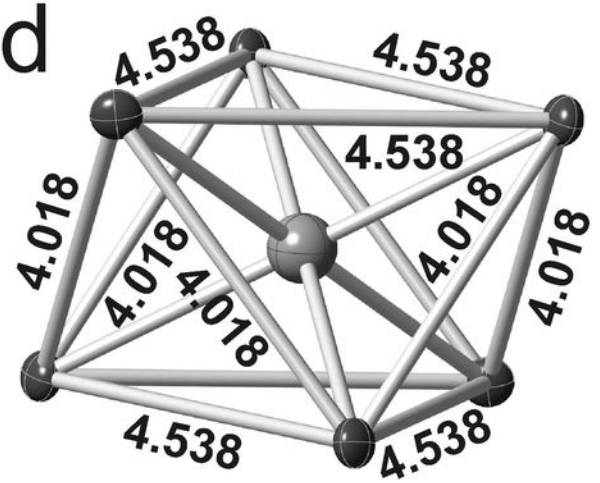
4.538
4.538
4.538
4.018
4.018
4.018
4.018
4.018
4.018
4.538
4.538